A conceptual design tool to support high-speed vehicle design

A conceptual design tool to support high-speed vehicle design

Davide Ferretto , Roberta Fusaro and Nicole Viola
Politecnico di Torino, Torino, 10129, Italy

Abstract

This paper aims at presenting an integrated multidisciplinary methodology and the related software tool, called ASTRID-H, developed at Politecnico di Torino to support the conceptual and preliminary design phases of high-speed vehicles. Based on the experience in the development of innovative methodologies to cope with complex and highly integrated aircraft, ASTRID-H has been developed to guide students, researchers and engineers through the very first phases of the design of high-speed vehicles. ASTRID-H supports the users to move from the statistical evaluation of the guess data and the identification of the design space to the geometrical characterization of the vehicle guaranteeing a proper integration of the main subsystems. Already available and widely used mathematical models are here integrated in a new algorithm to face the complexity of the design of high-speed vehicles. In addition, the coefficients of the semi-empirical models that were not focusing on high-speed vehicles have been updated to widen classical theories to cover high-speed vehicles. The resulting implemented methodology allows the users to cope with complex multidisciplinary problems, which encompass a variety of interrelated disciplines and heterogeneous levels of fidelity. Furthermore, this paper reports the some of the main results achieved during the validation of the methodology thanks to the application to the STRATOFLY MR3 vehicle case study. STRATOFLY MR3 is a Mach 8 waverider configuration that stems from more than a decade of European research activities in the field of high-speed and currently under investigation in the Horizon 2020 STRATOFLY Project.

1. Introduction

Today, the rapid development of aerospace technologies makes high-speed civil transportation a reality, promising to shorten the travelling time of one order of magnitude. Moreover, as eluded in more than a decade of EC-funded studies 20[1], some innovative high-speed aircraft configurations have now the potential to assure an economically viable high-speed aircraft fleet. They make use of unexploited flight routes in the stratosphere, offering a solution to the presently congested flight paths while ensuring a minimum environmental impact in terms of emitted noise and green-house gasses, particularly during stratospheric cruise. In this context, the attention of the worldwide aerospace community is focusing on the development of high-speed aircraft, which will integrate these newly developed technologies to guarantee faster, safer and more environmentally sustainable future aviation. However, to achieve this goal and thus guaranteeing top-level performance, holistic design methodologies for high-speed aircraft shall be defined cope with the high level of integration of the airframe and crucial on-board subsystems, with the high number of disciplines and with the presence of innovative multifunctional subsystems. Only a dedicated multi-disciplinary integrated design approach could realize this, by considering airframe architectures embedding the propulsion systems as well as meticulously integrating crucial subsystems. In this context, benefitting of the longtime experience in developing methodologies to support conceptual and preliminary design of complex aerospace vehicles and integrated subsystems and on the basis of the proprietary software tool ASTRID, Politecnico di Torino is currently validating an upgraded version of the tool, called ASTRID-H, specifically devoted to high-speed vehicles applications.

ASTRID (Aircraft on-board Systems sizing and TRade-off analysis in Initial Design) is a proprietary tool of the research group of Politecnico di Torino and it has been developed for almost a decade through research activities, encompassing Master of Science and Doctoral Theses [2]. This tool allows to carry out the aircraft conceptual and preliminary design, the sizing and integration of subsystems for a wide range of aircraft, from conventional to innovative configurations, mainly in the subsonic and low supersonic speed regime. ASTRID has been validated through the application to various case-studies and recently it has been included within the Multidisciplinary Optimization Framework set up within the Horizon 2020 AGILE (Aircraft 3rd Generation MDO for Innovative Collaboration of Heterogeneous Teams of Experts) project [3] and it is currently used in the follow up H2020 AGILE 4.0. This paper aims at showing how ASTRID-H extends the domain of ASTRID to high supersonic and hypersonic regime, paving also the way for space related applications such as reusable access to space and re-entry systems. The capability of performing rapid vehicle prototyping of ASTRID-H is currently being validated within the H2020 STRATOFLY (Stratospheric Flying Opportunities for High-Speed Propulsion Concepts) project for supersonic and hypersonic flight regimes and it is currently assessed for reusable access to space and re-entry system in ESA-funded projects.

Finally, it is worth noticing that ASTRID-H currently consists of two main parts: a conceptual design module and a subsystems design module. However, this paper only deals with the aircraft conceptual design module.

After this brief introduction explaining the genesis of ASTRID-H, Section II describes the software architecture and its main capabilities. Subsequently, Section III presents the methodology and implemented routines laying behind the conceptual module of ASTRID-H, pointing out the most important differences with respect to the approaches used for traditional aircraft design. Then, Section IV summarizes the results of the application of ASTRID-H to the conceptual

design of STRATOFLY MR3 vehicle. Eventually, Section V summarizes and comments on the results of the application and presents ideas for further improvements.

2. ASTRID-H: tool architecture and main capabilities.

2.1. From ASTRID to ASTRID-H: two decades of aerospace research activities

From the implementation perspective, the very first version of ASTRID has been drafted at the beginning of the years 2000 and it was organized in a series of Excel files, with different aims: from the identification of the geometrical characteristics of the vehicle, to the definition of a preliminary mass breakdown of the vehicle, up to the design of each single subsystem. Then, with the increasing complexity of the sizing routines and with the aim of easing the exploitation of the tool from external users, a new version of the tool has been developed in Visual Basic, providing for the first time an appealing graphical user interface. This version of ASTRID was able to support the design of conventional and unconventional aeronautical vehicles, including homebuilt propeller driven airplane, single engine propeller driven airplane, twin engine propeller driven airplane, agricultural airplane, Business Jet, regional turbo/propeller driven airplane, transport jet, military trainer, fighters, military patrol, bomb and transport airplane, flying boat, amphibious and float airplane, supersonic cruise airplane. However, more recently, the need of integrating the design of high-speed vehicles, characterized by highly innovative and complex concepts, requires an in-depth revision of the design routines as well as of the entire conceptual design process. The increased level of complexity and the need of combining design activities together with parallel simulation at different design levels (system, subsystem and component levels), strongly pushed towards the adoption of the implementation in a Matlab environment. In particular, to ease the tool deployment and to increase the number of users, ASTRID-H is currently developed and distributed as a web application. Besides the heritage, ASTRID-H covers a different range of vehicles, specifically focusing on High Speed transportation systems, including supersonic and hypersonic cruisers, suborbital vehicles and reusable access to space and re-entry systems.

2.2. ASTRID-H: a paradigm shift in aircraft design

ASTRID-H aims at providing a valuable support for the design of high-speed vehicles and related subsystems, thus encompassing both the conceptual and preliminary design phases, respectively. Furthermore, considering that feasible high-speed vehicle design can only be achieved thanks to a high level of integration between the airframe and the most impacting subsystems (e.g. the propulsion subsystem and the propellant subsystems, etc…), the aircraft conceptual design layer (namely Layer 0) and the subsystems preliminary design layer (Layer 1) are strictly interrelated (see Fig. 1). The fact that conceptual and preliminary design activities cannot anymore be carried out in series [4] represents a paradigm shift in aircraft design. Designers of high-speed vehicles cannot start from defining performant aerodynamic shapes to then just fitting the main subsystems inside the airframe. Conversely, the airframe shall be designed to wrap all the most important subsystems, thus the aircraft external layout usually results in being the best compromise between aerodynamic, thermal, propulsive performance and volumetric efficiency.

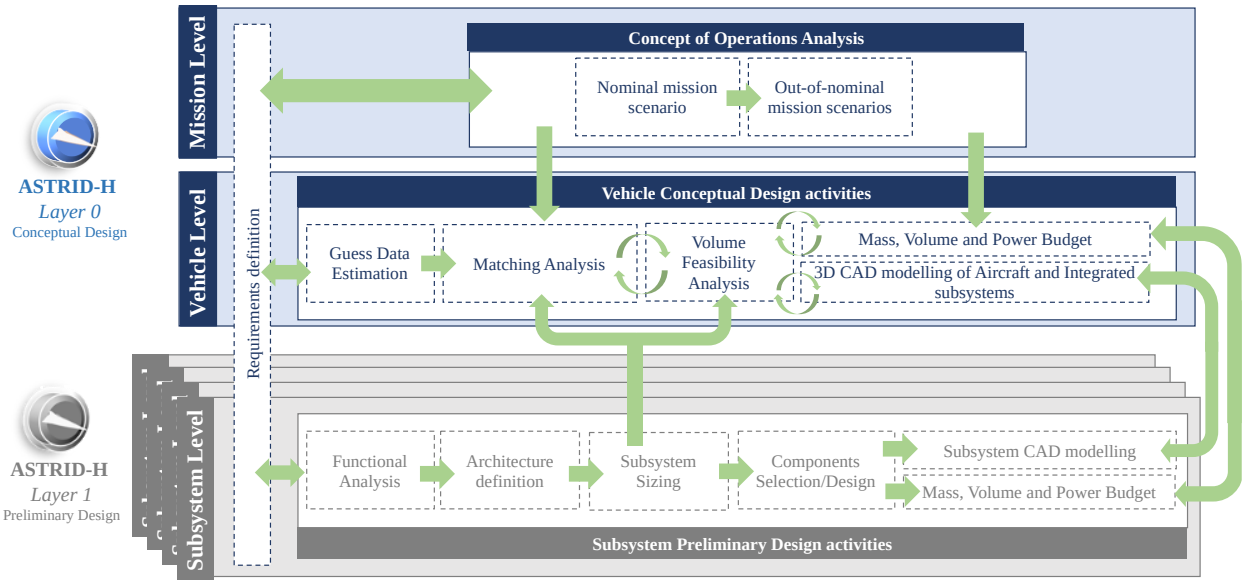

Fig. 1: ASTRID-H Architecture

Therefore, to implement a rapid but reliable aircraft conceptual design process, the definition of the general layout of the aircraft cannot prevent from being anticipated and supported by a detailed aircraft general performance analysis as well as from the design and sizing of the main subsystems. However, the final goal of the conceptual design phase remains the same: providing an assessment of the feasibility of vehicle and mission concepts from both the technical and operational standpoints. Many best practices and guidelines for aircraft conceptual design are available in literature [4], [5], [6] , suggesting typical workflows to draft a vehicle configuration and to evaluate the impact of requirements on the vehicle architecture and performance. In these processes, special attention is devoted to the identification or development of tools able to depict the design space at a glance, meeting stakeholders' expectations with design feasibility criteria [7][8]. For high-speed vehicles, the proper definition of the basic performance (e.g. mass, thrust and lifting surface) is crucial for the selection of a reference design point (or a region of points) to be considered as the baseline for the next development phases. However, to estimate the aircraft basic performance and geometrical parameters it is fundamental to properly define the design problem, compiling an exhaustive list of requirements and constraints and to preliminarily sketch the nominal mission profile. From the list of high-level requirements, criteria for the selection of an adequate statistical population are derived, paving the way for the estimation of the first guess data. Guess data are then used to start the design process. In details, the Conceptual Design Module of ASTRID-H consists of five complementary routines: Guess Data Estimation Routine, the Matching Analysis, the Volume Feasibility Analysis, the Mass and Volume Breakdown and the 3D CAD modelling of the aircraft and integrated subsystems (that is not dealt with in details in this paper).

3. ASTRID-H: tool architecture and main capabilities.

This section focuses on the description of the methodology implemented within the Layer 0 of ASTRID-H, and specifically on the conceptual design of high-speed aircraft. The module of ASTRID-H is thought to guide engineers in a step-by-step approach, providing feasible results in a fast and reliable way. The following subsections describe into the details each main routine of ASTRID-H Layer 0.

3.1. Guess Data Estimation

Traditional aircraft design methodologies have their starting point in the identification of a reference aircraft to be used as benchmark throughout the design process. However, this is not applicable in general for the design of breakthrough and innovative concepts, like in the case of high-speed aircraft. However, at the beginning of the process, once the high-level requirements are elicited, it is fundamental to make some preliminary hypotheses on the most important design and performance variables. To avoid the arbitrary assignment of values to these guess data, a structured approach is here proposed. Regression lines are built and used to set the initial numerical values of the guess variables but, of course, the scarce population of meaningful elements might prevent from a widespread exploitation of trends and forecasts. In case of breakthrough concepts and technologies, statistics can only be used to provide the users with an idea of where the project might stand in the envisaged scenario and to derive first attempt values for the guess data, with the possibility of envisaging new trends blooming. To cope with this activity, the Guess Data Estimation routine implemented in ASTRID-H consists of two algorithms:

- Algorithm A: Statistical analysis of high-speed vehicles. This algoritm is based on the exploitation of a high-speed vehicle database (encompassing already existing vehicles as well as demonstrators or simply conceptual studies), allowing for a pure statistical estimation of Guess Data (i.e. Operative Empty Mass m_{OE}, Fuel Mass m_f , Wing Planform Area S_{plan}, Engine Thrust T, Specific Impulse I_{sp} and/or Specific Fuel Consumption sfc). High Level Requirements are used as filtering criteria for the selection of a meaningful and homogeneous statistical population, allowing for quite accurate and realistic results. One of the main advantages of this approach is the fact that it can be initiated with a very narrow set of inputs, since the requirement on payload mass is sufficient to kick off the routine. Of course, the accuracy of the results is strictly related to the available population and this can lead to not very accurate results when dealing with very innovative vehicle or mission concepts.
- Algorithm B: Upgraded semi-empirical models for mass estimation of high-speed vehicles. This second algorithm still makes use of the statistical population but with a different scope: to upgrade already existing semi-empirical correlations to have a more accurate and reliable estimation of the Operative Empty Weight, the Fuel mas and the Maximum Take Off Weight. In details, thanks to a dedicated research activity, a set of already existing semiempirical models have been revised and new coefficients have been arranged to specifically cope with the different categories of high-speed vehicles. Differently from Algorithm A, this routine requires a wider input dataset, but the expected accuracy of the results is higher.

The diversity and complementarity of the two algorithms, provide the Guess Data Estimation routine of ASTRID-H with a multi-fidelity level characteristic. Indeed, both the implementation schemes reported in Fig. 2 are implemented and can be used. In case the user has a meager input dataset and simply knows the high-level requirements, the implementation scheme reported in Fig. 2 (left) shall be adopted. The small input dataset is used to execute Algorithm A

and subsequently, the outcomes of Algorithm A together with additional information, which becomes available from the user, feed Algorithm B. This procedure is iterated up until the convergence between the results of Algorithm A and B is reached. Complementary, the second implementation scheme, reported in Fig. 2 (right) can be used when the user has an ampler and more elaborated input dataset that enables the direct execution of Algorithm B. In this case, Algorithm A runs in parallel to Algorithm B to allow for a cross-check validation of the final results. In this case, the procedure is also iterated up until convergence between the results of Algorithm A and B is reached.

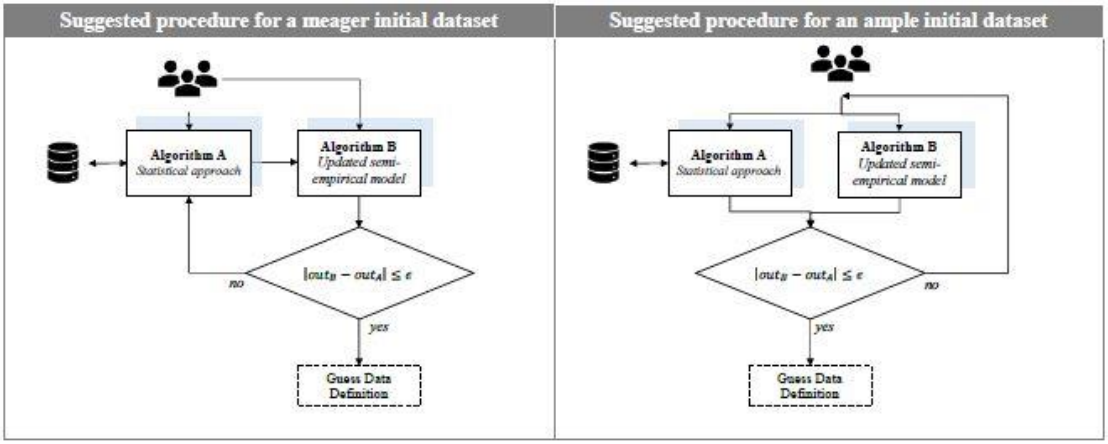

Fig. 2: ASTRID-H Guess Data Estimation Routine. Suggested procedure for a meager (left) and an ample (right) initial dataset

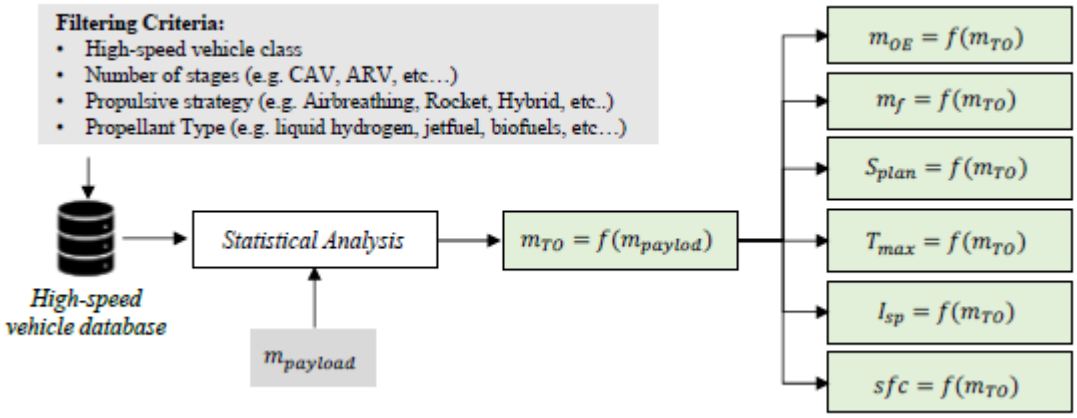

Fig. 3: ASTRID-H Guess Data Estimation Routine. Details on Algorithm A.

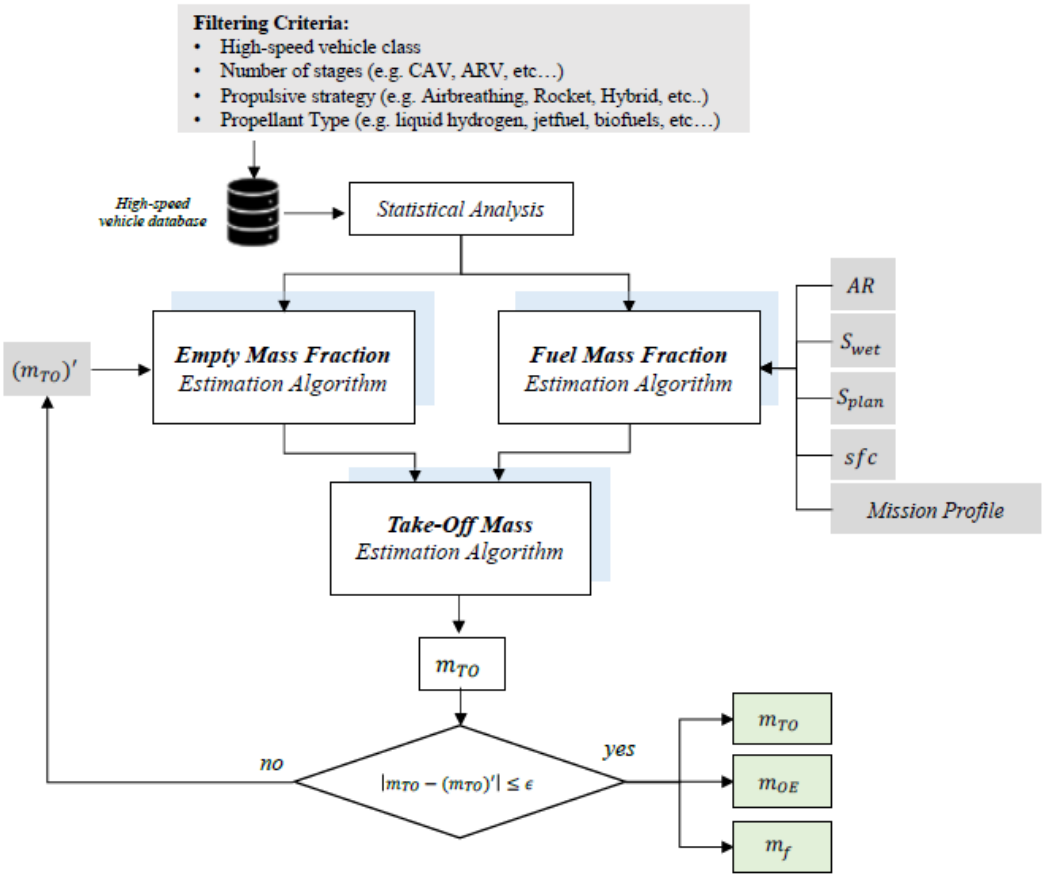

Fig. 4: ASTRID-H Guess Data Estimation Routine. Details on Algorithm B.

Details on Algorithm A are reported in Fig. 3. Specifically, the Algorithm can be executed using the payload mass as first independent variable and gathering from the database all the data related to a population coherently selected to capture the vehicle class (Cruise and Acceleration Vehicle (CAV), Reusable Access to Space and Re-entry Vehicles, etc..), the type of propulsion system (airbreathing or rocket) and eventually the type of fuel (cryogenic, traditional jet-fuels, etc…). Then, the Maximum Take Off Weight (MTOW) is evaluated as a function of the Payload Mass. Consequently, all the other Guess Data are evaluated using the MTOW as independent variable. Complementary, details on Algorithm B are reported in Fig. 4. The Algorithm B consists of three main parts: the estimation of the ratio between the Operative Empty Mass and the Take Off Mass, the ratio between the Fuel Mass and the Take Off Mass and finally the estimation of the Take Off Mass.

The *estimation of the ratio between the Operative Empty Mass and the Take Off Mass* (Fig. 5) starts from the assumption of a plausible value of take-off mass and the vehicle characterization through the definition of the first two semiempirical coefficients (A, C). In this case, the model presented by Raymer [4] is updated, thanks to the statistical analysis of the high-speed vehicle population.

$$\frac{m_{OE}}{m_{TO}} = A \cdot m_{T0}^{C} \cdot K_{vs} \cdot K_{comp}$$

The equation proposed in Raymer [4] and reported above is still able to capture the behavior of high-speed vehicles if proper coefficients are adopted. In particular, for the case of CAV equipped with air-breathing engines, two different sets of coefficients have been derived, depending on the type of fuel exploited: for storable propellant (e.g. traditional jet-fuels) $A = 3.85$ and $C = -0.18$ while for cryogenic propellant (e.g. liquid hydrogen), $A = 3.19$ and $C = -0.14$.

For the K_{vs} (correction factor that takes account of the geometric and mass penalty of wing with variable sweep angle) and K_{comp} (correction factor that takes into account the mass reduction due to the exploitation of composite materials) coefficients, the suggestions originally provided in [4] are considered applicable for this case study. Thus, K_{vs}=1 for fixed wing sweep and K_{vs}=1.04 for variable sweep wing; K_{comp}=1 for traditional metallic structures and K_{comp}=0.95 for composite materials. Higher mass reduction margins are expected from the introduction of highly performant materials (e.g. new lightweight metallic alloys with a high resistance to heat flux and temperature).

The *estimation of the ratio between the Fuel Mass and the Take Off Mass is reported in* Fig. 6. The estimation algorithm starts from the user assumptions on the Aspect Ratio, the ratio between the wetted surface and the wing reference surface, the specific fuel consumption that has to be specified for the different mission phases and of course, a

simplified mission profile. At first, the maximum Aerodynamic Efficiency (corresponding to cruise condition for CAV) is evaluated using the following equation, proposed in [4] :

$$\left(\frac{L}{D}\right)_{max} = K_{LD} \cdot \sqrt{AR_{wet}}$$

This equation contains a semi empirical coefficient (K_{LD}) that has been specifically evaluated for high-speed vehicles. Due to the wide range of vehicle configurations, a variation ($9.71 \leq K_{LD} \leq 14.71$) for the coefficient is expected. For CAV vehicles, the K_{LD} coefficient can be derived as function of the Küchemann coefficient K_w [9] (details on the K_w are reported in the Volume Matching Analysis subsection):

$$K_{LD} = \sqrt{K_w}$$

In addition, to compute the maximum aerodynamic efficiency, the wetted aspect ratio (AR_{wet}) shall be estimated. This parameter is defined as the ratio of the "geometrical" aspect ratio and the ratio of wetted and planform area. From the $\left(\frac{L}{D}\right)_{max}$, both Best Range and Best Endurance efficiency values are derived. Then, the total fuel mass fraction is evaluated by multiplying together the estimation of the fuel mass fractions per each mission phase. The formulation reported in the following equation can be used:

$$\frac{m_f}{m_{TO}} = \frac{m_{TO} - m_{landing}}{m_{TO}} = 1 - \sum\left(\frac{m_{f_i}}{m_{f_{i-1}}}\right)$$

The fuel mass for Warm-up, Take-off, climb and landing phases, at this stage, are evaluated on statistical bases. The following fuel fractions have been evaluated: 0.97 for warm-up and take-off, 0.55 for a climb phase a 0.995 for the landing phase. It is worth noticing that the value of the coefficient for the climb phase can be estimated as function of Mach in cruise phase, keeping in mind that the relationship between cruise Mach number and cruise altitude. All other fuel mass fractions are evaluated according to the Breguet equation.

Finally, the *estimation of the take-off mass* is performed. Using the m_{OE}/m_{TO} and m_f/m_{TO} ratios obtained from the previous sections, the gross take-off mass can be found iteratively. Design take-off mass (m_{TO}) can be broken down into Crew mass (m_{crew}), Payload mass ($m_{payload}$), Fuel mass (m_f), Empty mass (m_{OE}).

As summarized in Fig. 4, this algorithm is iterated, re-evaluating the ratio between the Operative Empty Mass and the Maximum Take Off Mass by updating the first attempt guess value of Maximum Take Off Mass. The iteration process ends when a convergence value for m_{TO} is reached. It is worth noticing that this final iterating cycle does not include a variation of the m_f/m_{TO} ratio, assuming that the iteration focuses only on the mass of the vehicle without any aerodynamic changes and thus keeping the same aerodynamic efficiency. However, all the values hypothesized or evaluated in this Guess Data Estimation routine shall be considered as first attempt values to be refined in the next iterative steps.

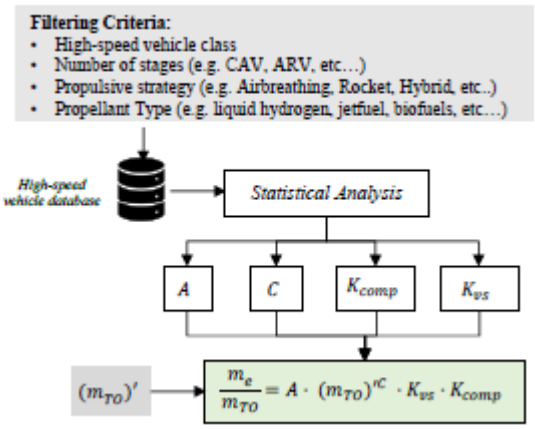

Fig. 5: Algorithm for the estimation of the ratio between Operative Empty Mass and the Take Off Mass

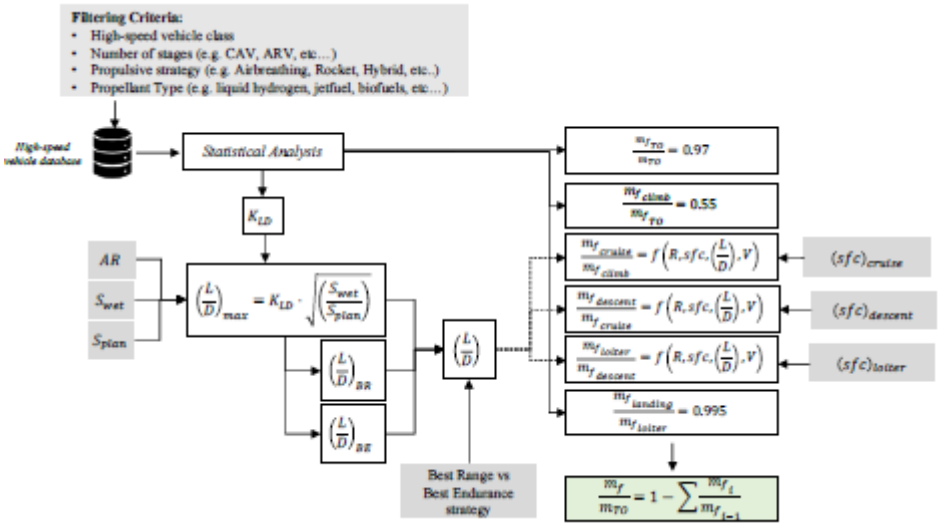

Fig. 6: Algorithm for the estimation of the ratio between Fuel Mass and the Take Off Mass

3.2. Design Space Definition: Matching Analysis and Volume Feasibility Analysis

The Matching Analysis and the Volume Feasibility Analysis represent the core of ASTRID-H Layer 0 because they guide the users from the preliminary guess data estimation to the definition of a feasible design space and the subsequent identification of an optimal design point. At this purpose, this Section consists of three different parts: in the first part, four different methods for the Aerodynamic preliminary characterization of high-speed vehicles are presented; the second part describes the complex algorithm set up for the definition of the design point, guaranteeing the feasibility in terms of performance and volume availability; finally the third part presents the Multiple Matching Chart approach to allow verifying that the evaluated design point belongs to the design space and suggesting paths to move towards the optimal design point.

High-speed vehicle Aerodynamic preliminary characterization

This routine aims at preliminary describing the aerodynamic behavior of high-speed vehicles throughout the mission profile, encompassing the subsonic ($0 \leq Mach \leq 0.9$), the transonic ($0.9 \leq Mach \leq 1.2$), the supersonic ($1.2 \leq Mach \leq 5$) and the hypersonic ($5 \leq Mach \leq 20$) speed regimes. Considering the lack of close analytical formulations for the aerodynamic characterization of the vehicle in the transonic regime and considering the very short duration of this condition, the estimation of specific aerodynamic coefficients for the transonic regime is neglected. Moreover, the willingness to guarantee a multi-fidelity tool and to support a wide spectrum of users and applications, four different aerodynamic models are implemented. However, it is worth noticing that even the simpler evaluation contains direct relationships with the aircraft minimum requested internal volume, thus unavoidably showing the strict relationship of the conceptual design with the design and sizing of the main subsystems. This prevents from the identification of optimal and highly performant aerodynamics layouts, which are not feasible from the volumetric standpoint. Details about the implemented models are hereafter reported, in an increasing order of complexity.

- *Aerodynamic Model 1 (modified Taylor Model)*. This aerodynamic model is a straightforward and simple way that allows the users to obtain an easy and fast estimation of the external aerodynamics of a high-speed aircraft in a conceptual design phase. In particular, the model is based on the correlation proposed in 1960 by Dwight Taylor [10]:

$$F = \sqrt{\left(\frac{V_{tot}}{S_{pln}^{1.5}}\right)^{0.66} \cdot \left(\frac{S_{wet}}{S_{pln}}\right)^{1.5}} = \tau^{0.333} \cdot K_W^{0.75}$$

This Equation makes use of already available guess data: the total aircraft volume V_{tot}, the aircraft planform area (also known as reference area) S_{plan} and the aircraft wetted surface S_{wet}. The combination of these design variables can also be expressed using two main parameters, K_W and the Küchermann's $\tau = \left(\frac{V_{tot}}{S_{pln}^{1.5}}\right)$. The complete model is reported in Table I, together with suggestions for the estimation of a new set of semi-empirical coefficients to widen the applicability of the Taylor Model for high-speed vehicles. Summarizing, the modified Taylor Model requires very few inputs and guarantees fast processing and it allows for the characterization of three mission parts. Conversely, results might be quite inaccurate considering that the vehicle customization is limited to the identification

of a proper Küchemann's τ and the obtained aerodynamic coefficients are not function of the Mach number and the aerodynamic incidence. However, this method can be used for the very first design iterations, when very few input data are available.

Table I: Mathematical Model of the Aerodynamic Model I

Aerodynamic Model I	
Lift Coefficient	$C_L \cong h \cdot (C_L)_{\frac{L}{D}max}$ [11] Where $\left(\frac{L}{D}\right)_{max} = \frac{a}{M} \cdot (M + b) \cdot (c - d \cdot F)$ [9] • semi-empirical coefficients *a*, *b*, *c* and *d* for CAV have been statistically evaluated as $a = 3.063$, $b = 3$, $c = 1.11238$ and $d = 0.1866$. • semi-empirical coefficient h has been derived for a CAV vehicle for three main mission phases: Acceleration (that might be representative of all climb phases and the first part of the cruise), Minimum Fuel Flow Cruise (representative of the cruise phase at constant speed) and Maximum Efficiency glide (representative of descending phases). In details, for the acceleration phase $h = 0.1$, for the Minimum fuel flow cruise phase $h = 0.82$ and for the Maximum efficiency glide $h = 1$.
Drag Coefficient	$C_d = i\, C_{d_0}$ Where $C_{D_0} = \frac{f \cdot e^{g \cdot F}}{\sqrt{M^2 - 1}}$ • semi-empirical coefficients f and g have been estimated for CAV as follows: $f = 0.05772$ and $g = 0.4076$. • semi-empirical coefficient i has been derived for a CAV vehicle for three main mission phases: for the acceleration phase $i = 1.075$; for the Minimum fuel flow cruise phase $i = 1$ and for the Maximum efficiency glide $i = 2$.

- <u>*Aerodynamic Model II (all-body hypersonic aircraft)*</u>. This model refers to a specific geometrical configuration, which is a delta planform with an elliptical cone forebody and elliptical cross-section afterbody, that forms a smooth transition surface from the end of the forebody to a straight-line leading edge. The aerodynamic method is simplified to a preliminary design level but includes all the main parts of the aircraft, namely wing, fuselage and fins. Geometry is defined by three independent parameters: the sweepback of the body leading edge, Λ; the position of the breakpoint between the forebody and afterbody, expressed as the breakpoint length ratio, $\frac{l_\pi}{l}$; the fatness ratio, specified as the ratio of the maximum cross-section area to the total planform area, $\frac{S_\pi}{S}$. To simplify the mathematical formulation and to guarantee the possibility of easily parametrize the results, the forebody ellipse ratio is used as main design variable (see Fig. 7):

$$\frac{a}{b} = \frac{\pi \cdot \left(\frac{l_\pi}{l}\right)^2 \cdot \cot\Lambda}{\frac{S_\pi}{S}}$$

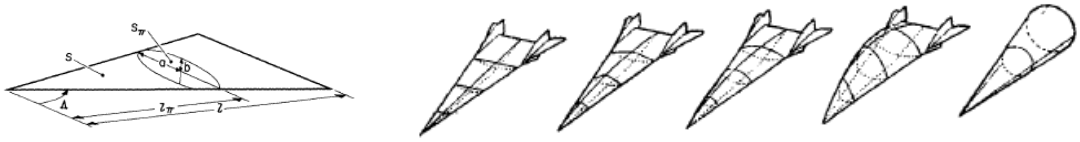

Fig. 7: All-body geometry parametrization [9]

Lift coefficient equation for this model are developed by curve fitting data for low aspect ratio wings from various references and applying Gothert's rule [12] or shock-expansion theory, where possible. The coefficients used in these equations have been modified to account for the rounded leading edge of the all-body configuration, which causes linear subsonic variation of the elliptic-cone lift coefficient as opposed to the significant nonlinear variation present for the sharp leading edge of a delta wing. The complete mathematical model is reported in Table II.

This model correctly captures some important aerodynamics characteristics of this type of vehicles. Firstly, it correctly shows how, in transonic and low supersonic Mach numbers, the pressure drag of the body is the dominant drag contributor. Secondly, the model predicts a reduction of pressure drag in the supersonic phase, while at hypersonic speeds, the body drag due to pressure and skin friction may equal the value from fin and form drag, in case of not highly slender body. Typically for highly slender bodies, usually selected as CAV, the most significant contributor to drag in hypersonic regime is the body skin friction drag.

Table II: Mathematical Model of the Aerodynamic Model II

<table>
<tr><th colspan="4">Aerodynamic Model II</th></tr>
<tr><td rowspan="2">Lift Coefficient</td><td colspan="3">$\boldsymbol{C_L = C_1 \cdot \sin\alpha + C_2 \cdot \sin^2\alpha}$</td></tr>
<tr><td>$\boldsymbol{M \leq 1}$ (subsonic flight regime)

$\boldsymbol{M > 1\ and\ \beta < \frac{4}{AR}}$
(supersonic flight regime)
$\boldsymbol{M > 1\ and\ \beta \geq \frac{4}{AR}}$
(hypersonic flight regime)</td><td>$C_1 = \frac{\pi \cdot AR}{2} - 0.0355 \cdot \beta^{0.45} \cdot AR^{1.45}$

$C_1 = \frac{4.17}{\beta} - 0.13$

$C_1 = \frac{\pi \cdot AR}{2} - 0.153 \cdot \beta \cdot AR^2$</td><td>$C_2 = 0$

$C_2 = bridge\ function$

$C_2 = e^{0.955 - \frac{4.35}{M}}$</td></tr>
<tr><td rowspan="3">Drag Coefficient</td><td colspan="3">$\boldsymbol{C_D = C_{D_0} + C_{D_i}}$
Zero-Lift (Parasite) Drag
$C_{D_0} = C_{D_{0_B}} + C_{D_{0_f}}$
• $C_{D_{0_B}}$ is the body contribution to the zero-lift drag coefficient.
• $C_{D_{0_f}}$ is the fins contribution to the zero-lift drag coefficient.</td></tr>
<tr><td colspan="3">Body Contribution
$C_{D_{0_B}} = C_{D_{p_B}} + C_{D_{F_B}} + C_{D_{B_B}}$
• $C_{D_{p_B}}$ is the body pressure drag coefficient. For CAV, the pressure drag is assumed zero. Indeed, a small effect can be accounted for in subsonic phases but considering the short time duration of subsonic mission phases for a CAV, this term can be neglected.
• $C_{D_{F_B}} = 0.455 \cdot \frac{\left[1+2\cdot\left(\frac{t}{c}\right)_{body}\right]\cdot\left(\frac{S_{wet}}{S_{pln}}\right)}{\left[\log_{10}(Re_{body})\right]^{2.58}\cdot\left(1+\frac{\gamma-1}{2}\cdot M_0^2\right)^{0.467}}$ is the body friction drag, where:
○ $Re_{body} = \rho_0 \cdot M_0 \cdot a_0 \cdot \frac{MAC_{body}}{\mu_0}$
○ $\left(\frac{t}{c}\right)_{body} = \frac{2\cdot\frac{l_\pi}{l}}{\frac{a}{b}\cdot\tan\Lambda}$
• $C_{D_{B_B}}$ is the body form drag. For CAV, experimental test campaigns revealed that this contribution is neglectable in subsonic regime due to the minimum heat flow that occurs in this condition, while it can be present in hypersonic regime in case of non-slender body shapes.
•</td></tr>
<tr><td colspan="3">Fins Contribution
$C_{D_{0_F}} = C_{D_{p_F}} + C_{D_{F_F}} + C_{D_{B_F}}$
• $C_{D_{p_F}}$ is the fin pressure drag coefficient. M_{SA} is the Mach number for shock attachment to leading edge.
$\begin{cases} C_{D_{p_F}} = 0 & M \leq 0.8 \\ C_{D_{p_F}} = bridge\ function & 0.8 < M < 1 \\ C_{D_{p_F}} = 3.4 \cdot \left(\frac{t}{c}\right)_{fin}^{\frac{5}{3}} \cdot \frac{S_{fin}}{S_{pln}} \cdot \cos^2\Lambda_{fin} & M = 1 \\ C_{D_{p_F}} = bridge\ function & 1 < M < M_{SA} \\ C_{D_{p_F}} = 6 \cdot \left(\frac{t}{c}\right)_{fin}^2 \cdot \frac{1}{\beta} \cdot \frac{S_{fin}}{S_{pln}}\ for\ M \geq M_{SA} \end{cases}$</td></tr>
</table>

	Where M_{SA} is the Mach number for shock attachment to leading edge. • $C_{D_{F_F}}$ is the fin friction drag $C_{D_{F_F}} = 0.455 \cdot \frac{\left[1+2\cdot\left(\frac{t}{c}\right)_{fin}\right]\cdot\left(\frac{S_{wet_{fin}}}{S_{pln}}\right)}{\left[Log(Re_{fin})\right]^{2.58}\cdot\left(1+\frac{\gamma-1}{2}\cdot M_0^2\right)^{0.467}}$, where $Re_{fin} = \rho_0 \cdot M_0 \cdot a_0 \cdot \frac{MAC_{fin}}{\mu_0}$ • $C_{D_{B_F}}$ is the fin form drag, and can be evaluated knowing the fin span and the fin leading edge radius $r_{LE_{fin}} = \left(0.725 \cdot \cos^{1.2}\Lambda_{fin}\right)^2 \cdot r_{nose}$ $$\begin{cases} C_{D_{B_F}} = 0 & M \le 0.8 \\ C_{D_{B_F}} = bridge\ function & 0.8 < M < M_{SA} \\ C_{D_{B_F}} = \frac{8}{3}\cdot\frac{r_{LE_{fin}}\cdot b_{fin}}{S_{pln}}\cdot\cos^2\Lambda_{fin} & M \ge M_{SA} \end{cases}$$
	Induced Drag $$C_{D_i} \approx C_{D_{i_B}} = K_M \cdot C_L \cdot \tan\alpha$$ Where the equation for the sharp leading-edge delta wing has been modified by introducing a semi-empiric coefficient that accounts for rounded leading edges [12] $$\begin{cases} K_M = 0.25\cdot(1+M) & for\ M < 3 \\ K_M = 1 & for\ M \ge 3 \end{cases}$$

- <u>*Aerodynamic Model III (Build-up approach)*</u>. This third Aerodynamic Model [4] is the most complete and it is able to provide more accurate results with respect to the previous methods. However, the higher level of completeness and accuracy is reflected into a more complex model that requests a consistent amount of inputs. The mathematical details are reported in Table III.

Table III: Mathematical Model of the Aerodynamic Model III

Aerodynamic Model III	
Lift Coefficient	***Subsonic regime*** $$C_L = C_{L_\alpha}\cdot\alpha$$ where $$C_{L_\alpha} = \frac{2\pi\cdot AR}{2+\sqrt{4+\frac{AR^2\beta^2}{\eta}\cdot\left(1+\frac{\tan^2\Lambda}{\beta^2}\right)}}\cdot\frac{S_{pln}}{S_{ref}}\cdot\mathcal{F}$$ Where AR is the wing geometric aspect ratio of the complete aircraft; $\beta = \sqrt{1-M^2}$ is the Prandtl-Glauert correction factor; $\eta = \frac{C_{L_\alpha}}{2\pi}$ is the wing profile efficiency; Λ is the sweep of the wing at the chord location where the airfoil is thickest; S_{pln} is the exposed wing planform (wing reference area less the part of the wing covered by the fuselage); F is the fuselage lift factor, which takes into account the fact that the fuselage (which diameter is d) creates lift due to the spill-over of lift from the wing (which span is b). The following equation can be used to estimate the fuselage lift factor: $$\mathcal{F} = 1.07\cdot\left(1+\frac{d}{b}\right)^2$$
	Supersonic regime $$C_L = C_{L_\alpha}\cdot\alpha$$ where $$C_{L_\alpha} = \frac{4}{\sqrt{1-M^2}}$$

Hypersonic regime

$$C_L \approx 2 \cdot sin^2(\theta) \cdot \cos(\theta)$$

Where

$$\theta = \sin^{-1}\left(\frac{1}{M}\right)$$

Subsonic regime

$$C_D = C_{D_0} + C_{D_i} = C_{D_0} + K \cdot C_L^2$$

Parasite drag

$$C_{D_0} = \frac{\sum C_{F_i} \cdot FF_i \cdot Q_i \cdot S_{wet_i}}{S_{ref}} + C_{D_{misc}} + C_{D_{L\&P}}$$

Where,

- C_f is the flat-plate skin-friction drag coefficient and can be estimated as follows:
  - For laminar flows ($Re \leq 5 \cdot 10^5$): $C_f = \frac{1.328}{\sqrt{Re}}$
  - For turbulent flows ($Re > 5 \cdot 10^5$): $C_f = \frac{0.455}{(\log Re)\text{^}2.58+(1+0.144\cdot M^2)\text{^}0.65}$

- FF is the form factor, which estimates the pressure drag due to viscous separation. The following simplified formulations can be adopted:
  - Wing, tail, strut, pylon (for a tail surface with hinged control surface, set about 10% higher form factor):

$$FF = \left[1 + \frac{0.6}{\left(\frac{x}{c}\right)_m} \cdot \left(\frac{t}{c}\right) + 100 \cdot \left(\frac{t}{c}\right)^4\right] \cdot [1.34 \cdot M^{0.18} \cdot (\cos\Lambda)^{0.28}]$$

  - Fuselage and smooth canopy:

$$FF = 0.9 + \frac{5}{f^{1.5}} + \frac{f}{400}$$

  - Nacelle and smooth external store:

$$FF = 1 + \frac{0.35}{f}$$

  - Jet inlet (double wedge diverter)

$$FF = 1 + \frac{d}{l}$$

  - Jet inlet (single wedge diverter)

$$FF = 1 + \frac{2d}{l}$$

Where $\frac{t}{c}$ is the profile thickness on chord ratio; $\left(\frac{x}{c}\right)_m$ is the chordwise location of the airfoil maximum thickness point (typically 0.3 for low-speed airfoil, or 0.5 for high-speed profiles) and $f = \frac{l}{d} = \frac{l}{\sqrt{\frac{4}{\pi}AR}}$

- Q is the interference effect on the component drag; $C_{D_{misc}}$ is the miscellaneous drags for special features of an aircraft such as flaps, un-retracted landing gear, an upswept aft fuselage, and base area, and $C_{D_{L\&P}}$ is the contribution for leakages and protuberances. Typical values suggested by Raymer can be adopted.

Induced drag

$$K = \frac{1}{\pi \cdot AR \cdot e}$$

Where the extra drag due to nonelliptical lift distribution and the flow separation are taken into account from the Oswald efficiency factor; this is typically in the range

$$0.7 \leq e \leq 0.85$$

It is otherwise possible to estimate the value of e through some semi-empirical equations [4]

- straight wing

$$e = 1.78 \cdot (1 - 0.045 \cdot AR^{0.68}) - 0.64$$

- swept wing (if $\Lambda > 30°$)

$$e = 4.61 \cdot (1 - 0.045 \cdot AR^{0.68}) \cdot [\cos(\Lambda_{LE})]^{0.15} - 3.1$$

- swept wing (if $\Lambda < 30°$)
  linear interpolation between the previous two equations.

Supersonic Regime

$$C_{D_0} = \frac{\sum C_{F_i} \cdot S_{wet_i}}{S_{ref}} + C_{D_{wave}} + C_{D_{misc}} + C_{D_{L\&P}}$$

- C_f is the flat-plate skin-friction drag coefficient, (turbulent). The model reported in subsonic regime is still applicable.
- $C_{D_{wave}}$ is the wave drag component, which considers the pressure drag due to shock formation; This contribution is evaluated using a Sears-Haack body geometry that can be defined on the basis of the variation of the r is the cross-section radius and l is the longitudinal dimension $\left(-\frac{l}{2} \leq x \leq \frac{l}{2}\right)$

$$\frac{r}{r_{max}} = \left[1 - \left(\frac{2x}{l}\right)^2\right]^{0.75}$$

The wave drag, in this case, is obtainable from the following relation, as a function of the maximum cross-sectional area (A_{max})

$$\left(\frac{D}{q}\right)_{S-H} = \frac{9\pi}{2} \cdot \left(\frac{A_{max}}{l}\right)^2$$

The maximum cross-sectional area is determined from the aircraft volume distribution plot. For preliminary wave drag analysis, it is possible to use the following semi-empiric correlation to the Sears-Haack body wave drag, where E_{WD} is an empirical wave-drag efficiency factor and represents the ratio between actual wave drag and the Sears-Haack value. According to Raymer, for blended delta wing, E_{WD}=1.2, for supersonic aircraft $1.8 < E_{WD} < 2.2$. In case of not very efficient aerodynamic design, values greater than 2.5 can be adopted.

$$\left(\frac{D}{q}\right)_{wave} = E_{WD} \cdot \left[1 - 0.2 \cdot (M - 1.2)^{0.57} \cdot \left(1 - \frac{\pi \cdot \Lambda^{0.77}(\text{deg})}{100}\right)\right] \cdot \left(\frac{D}{q}\right)_{S-H}$$

- $C_{D_{misc}}$ is the miscellaneous drags for special features of an aircraft such as flaps, un-retracted landing gear, an upswept aft fuselage, and base area. The subsonic dissertation is still valid in supersonic regime; however, the formula for the base drag should be modified as follows:

$$\left(\frac{D}{q}\right)_{base} = [0.064 + 0.042(M - 3.84)^2] \cdot A_{base}$$

- $C_{D_{L\&P}}$ is the contribution for leakages and protuberances.

Induced drag

The only difference will be the equation used for the determination of the K factor, which is now function of the aspect ratio, Mach number and leading-edge sweep angle.

$$K = \frac{AR \cdot (M^2 - 1) \cdot \cos(\Lambda_{LE})}{4 \cdot AR \cdot \sqrt{M^2 - 1} - 2}$$

Hypersonic Regime

$$C_D = 2 \cdot sin^3(\theta)$$

- *Aerodynamic Model IV (AEDB from numerical or experimental activities)*. Thanks to this routine, ASTRID-H allows the expert users to see the impact of an already defined complete aerodynamic database on to the main aircraft design variables. In this case, the user can directly feed the Preliminary Design Point Estimation routine with the available results coming from numerical or experimental research activities.

Preliminary Design Point Estimation

This section of the paper aims at describing the algorithm that allows to make a first estimation of the design point on the basis of the dataset evaluated into the previous steps. Details of the implementation are reported hereafter. Starting

from the exploitation of one of the Aerodynamic models reported in the previous section, a new value for the fuel mass can be computed in a more accurate way with respect to the guess data estimation. Knowing the type of fuel to be used, the minimum requested volume for tanks is computed. At the same time, other already available inputs are called from the previous routines and here used to evaluate the following design parameters. In particular, the first parameter to be evaluated is the propulsion index (I_P) that can be expressed as a function of the maximum Mach number [11]

$$I_P = \frac{\rho_f}{m_R - 1} = 107.6 \cdot 10^{-0.081 \cdot M_{max}}$$

Where

$$m_R - 1 = \frac{m_f}{m_{OE} + m_{pay}}$$

The second important parameter is the Küchermann's τ, which is used extensively along this method; it expresses a relation between the operative empty mass and vehicle design parameters. It can otherwise be seen as a slenderness ratio $\left(\tau = \frac{V_{tot}}{S_{pln}^{1.5}}\right)$. Starting from the original work of Kückemann, the typical formulation of $K_w = \frac{S_{wet}}{S_{pln}}$ can be specialized for different vehicle classes, encompassing different types of propellant and propulsion strategies. In details, the following correlations can be used

$$\frac{K_w}{\tau} = e^{0.081 \ln(\tau)^2 - 0.461 \ln(\tau) + 1.738}$$

As it is reported in Fig. 8, the formulation is able to capture different vehicle configurations as well as different types of propellant.

The evaluation of the τ allows for the definition of other three important indexes:

$$K_v = \frac{V_f}{V_{tot}} \cdot S_{pln}^{-0.0717}$$

$$K_{str} = 0.228 \quad \cdot \tau^{0.2}$$

$$I_{str} = \frac{m_{str}}{S_{wet}} = \frac{K_{str} \cdot K_v \cdot \tau}{K_w} \cdot I_p \cdot \frac{S_{pln}^{1.5717}}{1 + \frac{m_{pay}}{m_{OE}}}$$

This means that given the propulsion and structural indexes, the vehicle size can be readily estimated as a function of τ, its geometrical configuration and payload mass, as follows

$$S_{pln} = \left[\frac{I_p}{I_{str}} \cdot \frac{K_w}{\tau} \cdot \frac{1}{K_v} \cdot \frac{1}{K_{str}} \cdot \left(1 + \frac{m_{pay}}{m_{OE} + m_{pay}}\right)\right]^{1.409}$$

Thanks to the introduction of these parameters, the operative empty mass estimation can now be refined using the following equation:

$$m_{OE} = \frac{V_f}{V_{tot}} \cdot \tau \cdot I_p \cdot S_{pln}^{1.5} \cdot \frac{1}{1 + \frac{m_{pay}}{m_{OE}}}$$

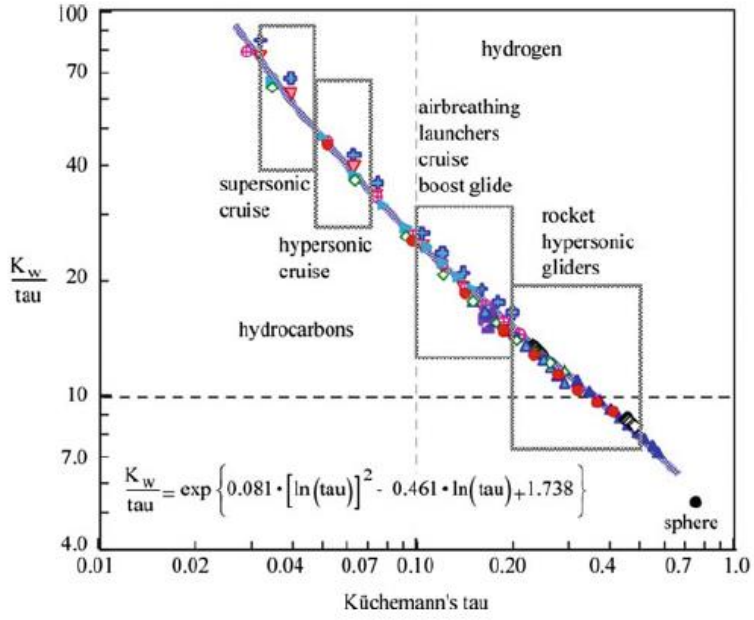

Fig. 8: Kückemann $\frac{K_W}{\tau}$ correlation [9]

This newly estimated value for the planform area can now be compared with the initial guess data and the routine is iterated up until convergence is reached. However, this set of iterations does not provide the design point yet. Indeed, it is necessary to verify if the evaluated surface and mass fulfil the two most stringent requirements on Wing Loading and Thrust to Weight ratio, i.e, the Take-Off and Landing Requirements. Mathematical details of these algorithms are reported in Fig. 8. If one of these two requirements is not fulfilled, a new iteration loop on the planform area is initiated. The iteration includes an update of the main aerodynamic coefficients.

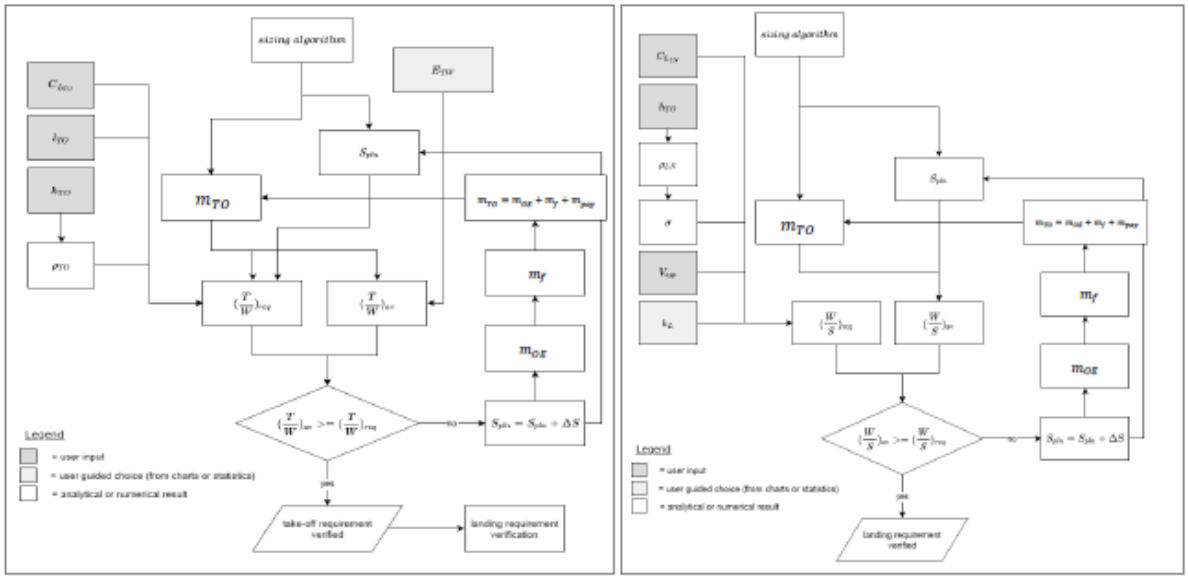

Fig. 9: Design point verification with respect to Take-off (left) and Landing (right) requirement

Matching Chart: design space verification and suggestion for the optimization

Once the design point is identified, ASTRID-H moves to the verification of where the design point stands within the design space. To pursue this goal, ASTRID-H implements the Multiple Matching Chart Approach already published by Politecnico di Torino in [13]. Matching Chart is one of the most widely used tool in conceptual design and it consists of a graphical representation of the different performance requirements (curves representing the Thrust-to-Weight ratio requirement as function of the Wing Loading) for each mission phase.

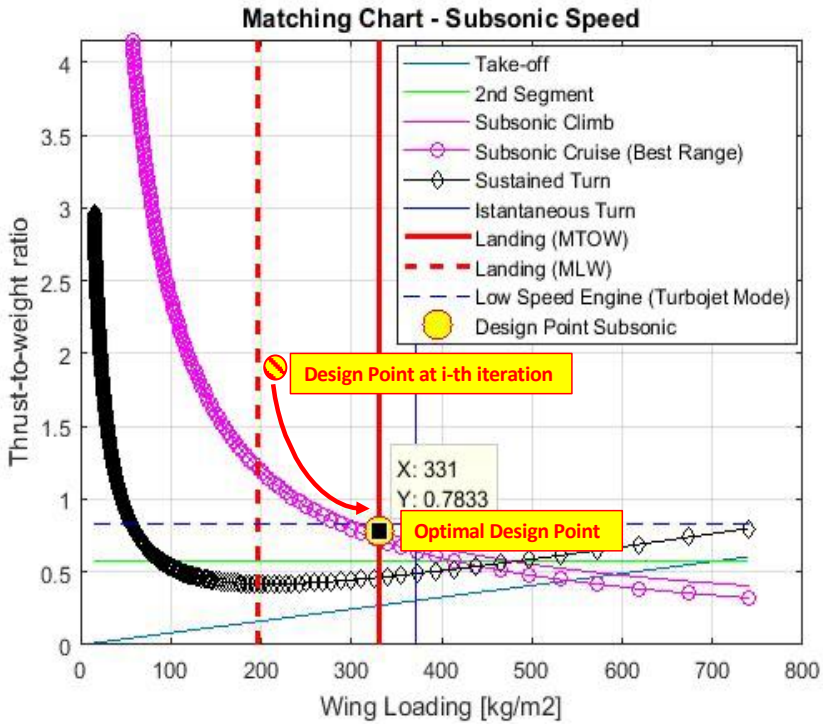

Fig. 10: Example of Aircraft Matching Chart for subsonic regime

The exploitation of this tool allows the identification of a feasible design space as well as the definition of a reference vehicle configuration in terms of maximum thrust, Maximum Take-Off Weight and wing surface since the very beginning of the design process. Although the tool was originally developed for conventional aircraft, several extensions and updates of the mathematical models have been proposed over the years to widen its application to innovative configurations. In particular, [13] presents a further evolution of the Matching Chart model to support the conceptual design of high-speed transportation systems, encompassing supersonic and hypersonic flight vehicles. An example of the result of the exploitation of this tool within the ASTRID-H Layer 0 is reported in Fig. 10. Specifically, this tool allows verifying if the design point is correctly located in the feasible region of the design space. Then, the tool suggests possible modifications to the design variables to move the design point closer to the optimal design condition. Currently this is not fully automatized, but the authors are working at it. Figure 10 shows the example of the Subsonic speed regime that is usually the most critical one, considering that it provides the most stringent requirements in terms of wing loading.

3.3. Mass and Volume Budget

Once the ASTRID-H Matching Chart and Volume Feasibility routines reach the convergence, the design point can be fixed. At this stage, the Mass and Volume Breakdown routine can be initiated providing the main mass and volume items. In details, Table IV and Table V report the mathematical model used for the mass and volume breakdown evaluations, respectively.

Please note that the values here suggested for the various coefficients come from [14] in which high number of high-speed vehicles are analyzed.

Table IV: Mass Breakdown Mathematical Model

Mass Breakdown Model	
Structural Mass (m_{str})	$$m_{str} = I_{str} \cdot K_w \cdot S_{pln} + m_{cprv}$$ Where: • I_{str} is the structural index. It is the ratio of structure weight and wetted area $I_{str} = \frac{W_{str}}{S_{wet}}$. Typical range for this coefficient is $17 \leq I_{str} \leq 23 \frac{kg}{m^2}$; • K_w is a configurational index. It is the ratio of wetted surface on planform area $K_w = \frac{S_{wet}}{S_{pln}}$. Typical range for this coefficient has been extensively discussed in the core sizing method paragraph; • m_{cprv} is the crew provision mass. It can be evaluated as follows $$m_{cprv} = f_{cprv} \cdot N_{crew}$$ Where:

	○ f_{cprv} is a crew mass index. It is the "crew member specific weight". Typical range for this coefficient is $450 \leq I_{str} \leq 500\,\frac{kg}{person}$; ○ N_{crew} is the number of piloting crew.
Engine Mass (m_e)	$$m_{eng} = \frac{\left(\frac{T}{W}\right)_{TO} \cdot \left(\frac{m_{TO}}{m_{OE}}\right)}{\left(\frac{T}{W}\right)_{E}} \cdot m_{OE}$$ • $\left(\frac{T}{W}\right)_{TO}$ is the engine thrust-to-weight ratio at take-off; • $\left(\frac{T}{W}\right)_{E}$ is the engine thrust-to-weight ratio, sea level static. Typical range for this coefficient is $12.5 \leq \left(\frac{T}{W}\right)_{E} \leq 17.5$.
Subsystems Mass (m_{subsys})	$$m_{subsys} = C_{sys} + f_{sys} \cdot m_{OE}$$ Where: • C_{sys} is a systems mass index. It is the "constant system weight". It can be evaluated as follows $$C_{sys} = C_{un} + f_{mnd} \cdot N_{crew}$$ Where: ○ C_{un} is a constant system parameter. It is the "unmanned system weight". Typical range for this coefficient is $1900 \leq C_{un} \leq 2100\ kg$; ○ f_{mnd} is a crew mass index. It is the "crew system specific weight". Typical range for this coefficient is $1450 \leq f_{mnd} \leq 1050\,\frac{kg}{person}$; ○ N_{crew} is the number of piloting crew. • f_{sys} is a systems mass index. It is the "variable system weight coefficient". Typical range for this coefficient is $0.16 \leq f_{sys} \leq 0.24\,\frac{kg}{kg}$.
Operative Empty Mass (m_{OE})	$$m_{OE} = m_{str} + m_e + m_{subsys}$$
Take-Off Mass (m_{TO})	$$m_{TO} = m_{OE} + m_{crew} + m_{pay} + m_f$$

Table V: Volume Breakdown Mathematical Model

Volume Breakdown Model	
Fuel Volume (V_f)	$$V_f = \frac{\frac{m_{TO}}{m_{OE}} - 1}{\rho_f} \cdot m_{OE}$$
Subsystems Volume (V_{subsys})	$$V_{subsys} = K_{vs} \cdot V_{tot} + V_{fix}$$ • K_{vs} is the "system volume coefficient". Typical range for this coefficient is $0.02 \leq k_{vs} \leq 0.04\,\frac{m^3}{m^3}$; • V_{fix} is the "fixed system volume", and it is accessory to the system volume to the complete definition of all on-board systems. It is mainly a function of the number of crew elements, as follows $$V_{fix} = V_{un} + f_{crw} \cdot N_{crew}$$ Where: ○ V_{un} is the "unmanned fixed system volume". Typical range for this coefficient is $5 \leq V_{un} \leq 7\ m^3$; ○ f_{crw} is the "crew member specific weight". Typical range for this coefficient is $11 \leq f_{crw} \leq 12\,\frac{m^3}{person}$; ○ N_{crew} is the number of piloting crew.
Engine Volume	$$V_{eng} = k_{ve} \cdot (T/W)_{TO} \cdot m_R \cdot m_e$$

(V_e)	Where: • k_{ve} is the "engine volume coefficient". Typical range for this coefficient is $0.25 \leq k_{ve} \leq 0.75 \frac{m^3}{thrust(ton)}$; • $(T/W)_{TO}$ is the engine thrust-to-weight ratio at take-off.
Empty Volume (V_{void})	$$V_{void} = k_{vv} \cdot V_{tot}$$ Where k_{vv} is the "void volume coefficient". Typical range for this coefficient is $0.1 \leq k_{vv} \leq 0.2 \frac{m^3}{m^3}$.
Payload Volume (V_{pay})	$$V_{pay} = \frac{N_{pax} m_{pax}}{\rho_{pay}}$$ Where: • N_{pax} is the total passengers number (consider the maximum possible load) • m_{pax} is the mass of a single passenger and its luggage. Typical value for this mass is $80\ kg$ for the person and $20\ kg$ for the luggage, hence $100 \frac{kg}{passenger}$ (to be conservative) • ρ_{pay} is the average payload density. For civil transport, a typical range for this coefficient is $48 \leq \rho_{pay} \leq 130 \frac{kg}{m^3}$.
Crew Volume (V_{crew})	$$V_{crew} = \left(k_{cprv} + k_{crew}\right) \cdot N_{crew}$$ Where: • k_{cprv} is the crew provision volume. A typical range for this coefficient $5 \leq k_{cprv} \leq 6 \frac{m^3}{person}$ • k_{crew} is the crew member volume. A typical range for this coefficient $0.9 \leq k_{crw} \leq 2 \frac{m^3}{person}$ • N_{crew} is the total crew members number (both piloting and flight attendants)
Total Volume (V_{tot})	$$V_{tot} = \tau \cdot S_{pln}^{1.5} = V_f + V_{sys} + V_e + V_{void} + V_{pay} + V_{crew}$$

3.4. Case studies description

This paper presents the application of ASTRID-H methodology and tool to the Cruise and Acceleration Vehicle. Considering the high level of complexity of this type of high-speed vehicles, only a dedicated multi-disciplinary integrated design approach could provide feasible results since the conceptual design phase. Indeed, it is essential to draft vehicle external layout by considering airframe architectures embedding the propulsion systems as well as meticulously integrating crucial subsystems. In particular, the STRATOFLY MR3 vehicle configuration and mission is here used as example. The vehicle is currently under investigation within the STRATOFLY project, funded by the European Commission, under the framework of Horizon 2020 plan, with the aim of assessing potential of this type of high-speed transport vehicle to reach TRL6 by 2035, with respect to key technological, societal and economical aspects, such as thermal and structural integrity, low-emissions combined propulsion cycles, subsystems design and integration including smart energy management, environmental aspects impacting climate change, noise emissions and social acceptance, and economic viability accounting for safety and human factors.

Specifically, STRATOFLY MR3 integrates 6 Air Turbo Rocket engines, ATR, that operate up to Mach 4-4.5 and one Dual Mode Ramjet, DMR, that is used for hypersonic flight from Mach 4.5 up to Mach 8. It is worth remembering that STRATOFLY exploits liquid hydrogen which guarantees the complete decarbonization, thus fulfilling another top mission requirement. Moreover, it can be easily verified that STRATOFLY MR3 vehicle is driven by its peculiar mission, which can be summarized as follows: STRATOFLY MR3 shall be able to fly along antipodal route (R > 16000 km) reaching Mach 8 during cruise at a stratospheric altitude (h > 30000 m) carrying 300 passengers as payload. Fig. 11 depicts the trajectory of STRATOFLY MR3. In addition, Fig. 12 shows current STRATOFLY MR3 external and internal layout.

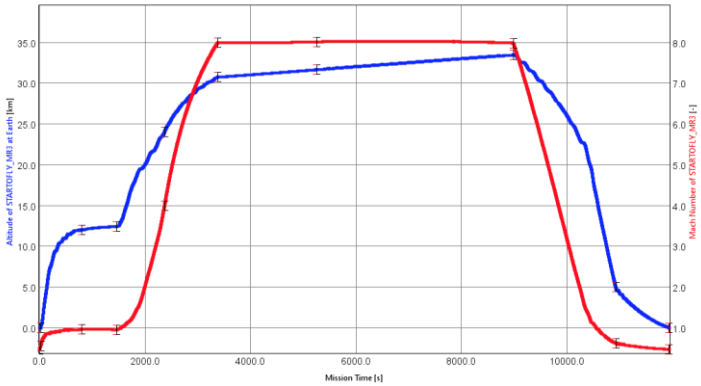

Fig. 11: STRATOFLY MR3 reference trajectory in terms of altitude versus time and Mach number versus time

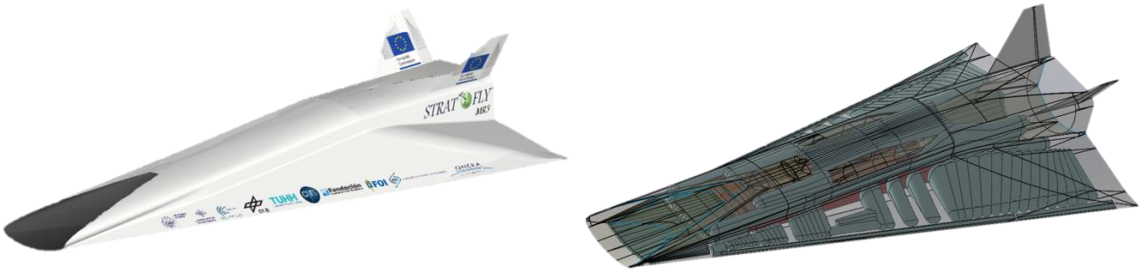

Fig. 12: STRATOFLY MR3 external and internal configuration

As already mentioned, STRATOFLY MR3 has a waverider configuration (Fig. 12) with the engines and related air duct embedded into the airframe and located at the top. The integration of the propulsive system at the top of the vehicle allows to maximize the available planform for lift generation without additional drag penalties and to optimize the internal volume. This layout guarantees furthermore to expand the jet to a large exit nozzle area without the need to perturb the external shape which would lead to extra pressure drag. Examples of results provided by ASTRID-H at the end of the Layer 0 iterations are reported hereafter, for this reference CAV vehicle (Fig. 13).

Table VI: Preliminary Results for the STRATOFLY MR3 vehicle case-study

Parameter	STRATOFLY MR3 by ASTRID-H	STRATOFLY MR3 Reference values	Differences
Required Wing surface [m^2]	>1110	1365	-18,7%
Take off mass [kg]	399,886	400,000	< 1%
Operative Empty Mass [kg]	219,146	190,000	+15.3%
Fuel Mass [kg]	150,740	180,000	-16.3%
Payload Mass [kg]	30,000 (input data)	30,000	N/A

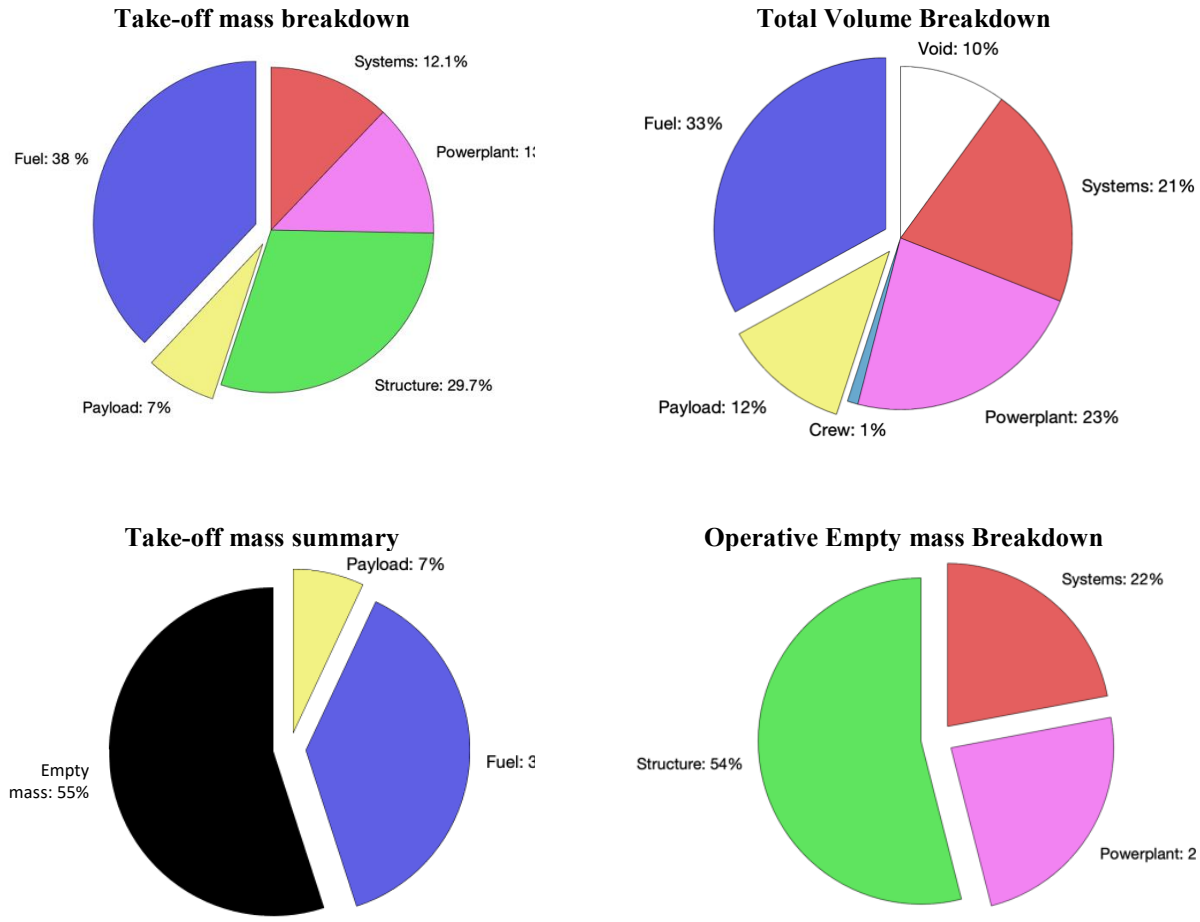

Fig. 13: STRATOFLY MR3 Mass and Volume Breakdown

4. Conclusions

This paper describes the design methodology developed by Politecnico di Torino and implemented within the proprietary tool ASTRID-H to support conceptual and preliminary design of a wide range of high-speed vehicles. Already available and widely used mathematical models have been here integrated in a new comprehensive algorithm to face the complexity of the design of high-speed vehicles. In addition, the coefficients of the semi-empirical models that were not focusing on high-speed vehicles have been updated to widen classical theories to cover high-speed vehicles.

Moreover, the paper describes the possibility to support a wide range of users allowing for a multi-fidelity exploitation of the tool. Indeed, depending on the available input dataset, the user can decide to follow a specific path exploiting those algorithms that best fit with the levels of details of the available input dataset.

The preliminary results reported in the previous section make evidence of the successful validation of the various routines and algorithms for the STRATOFLY MR3 vehicle. Looking at Table VI, the error margins are below the 20% and this is in line with the expectations of a conceptual design stage. In particular, throughout the paper, suggestions for the design of a CAV are reported and have been validated with the case study. However, the authors are working at improving all the routines to better capture the peculiarities of other high-speed vehicle classes, with specific focus on Reusable Access to Space and Re-entry vehicles.

Acknowledgement

The validation of ASTRID-H methodology and tool, that has been reported in this paper, has been achieved so far in the framework of the H2020 STRATOFLY Project. This project has received funding from the European Union's Horizon 2020 research and innovation programme under grant agreement No 769246 within the Stratospheric Flying Opportunities for High-Speed Propulsion Concepts (STRATOFLY) Project.

References

[1] Steelant, J., Varvill, R., Walton, C., Defoort, S., Hannemann, K., Marini, M.: Achievements Obtained for Sustained Hypersonic Flight within the LAPCAT-II project. In: 20th AIAA International Space Planes and Hypersonic Systems and Technologies Conference AIAA, Glasgow, AIAA-2015-3677, 6–9 July 2015

[2] S. Chiesa, G. A. Di Meo, M. Fioriti, G. Medici and N. Viola, "ASTRID - Aircraft On Board Systems Sizing and Trade-Off Analysis in Intial Design," in READ, Brno (CZ), 2012

[3] Prakasha, P.S., Ciampa, P.D., Boggero, L., Fioriti, M., Aigner, B., Mirzoyan, A., Isyanov, A., Anisimov, K., Kursakov, I., Savelyev, A. Collaborative system of systems multidisciplinary design optimization for civil aircraft: AGILE EU project (2017) 18th AIAA/ISSMO Multidisciplinary Analysis and Optimization Conference, 2017, 27 p.

[4] Raymer, Daniel. Aircraft design: a conceptual approach. American Institute of Aeronautics and Astronautics, Inc., 2012.

[5] Roskam, Jan. Airplane design. DARcorporation, 1985.

[6] Torenbeek, Egbert. Synthesis of subsonic airplane design: an introduction to the preliminary design of subsonic general aviation and transport aircraft, with emphasis on layout, aerodynamic design, propulsion and performance. Springer Science & Business Media, 2013.

[7] Fusaro, Roberta, Davide Ferretto, and Nicole Viola. "Model-Based Object-Oriented systems engineering methodology for the conceptual design of a hypersonic transportation system." 2016 IEEE international symposium on systems engineering (ISSE). IEEE, 2016. : 10.1109/SysEng.2016.7753175

[8] Fusaro, Roberta, Davide Ferretto, and Nicole Viola. "MBSE approach to support and formalize mission alternatives generation and selection processes for hypersonic and suborbital transportation systems." 2017 IEEE International Systems Engineering Symposium (ISSE). IEEE, doi 10.1109/SysEng.2017.8088275

[9] D. Kuchermann, The Aerodynamic Design of Aircraft, Blacksburg, Virginia: AIAA Education Series, 2012.

[10] C. B. B. C. P. A. Czysz, Future Spacecraft Propulsion Systems and Integration - Enabling Technologies for Space Exploration, Arlington, Texas: Springer, 2012.

[11] S. N. B. M. E. T. Curran, Scramjet propulsion, Cambridge, Massachusetts, 2000.

[12] L. J. Williams, «Estimated Aerodynamics of All-Body Hypersonic Aircraft Configurations,» National Aeronautics and Space Administration, Moffett Field, California, March 1971.

[13] Ferretto, Davide, Roberta Fusaro, and Nicole Viola. "Innovative Multiple Matching Charts approach to support the conceptual design of hypersonic vehicles." Proceedings of the Institution of Mechanical Engineers, Part G: Journal of Aerospace Engineering (2020): https://doi.org/10.1177/0954410020920037

[14] Chudoba, Bernd, Gary Coleman, Amit Oza, Lex Gonzalez, and Paul Czysz. "Solution-Space Screening of a Hypersonic Endurance Demonstrator." (2012).